

Anti-Windup Algorithms for Pilot-Induced-Oscillation Alleviation

Isabelle Queinnec, Sophie Tarbouriech, Jean-Marc Biannic, Christophe Prieur

▶ **To cite this version:**

Isabelle Queinnec, Sophie Tarbouriech, Jean-Marc Biannic, Christophe Prieur. Anti-Windup Algorithms for Pilot-Induced-Oscillation Alleviation. Aerospace Lab, 2017, 13, pp.AL13-07. 10.12762/2017.AL13-07 . hal-01636186

HAL Id: hal-01636186

https://laas.hal.science/hal-01636186

Submitted on 24 Nov 2017

HAL is a multi-disciplinary open access archive for the deposit and dissemination of scientific research documents, whether they are published or not. The documents may come from teaching and research institutions in France or abroad, or from public or private research centers.

L'archive ouverte pluridisciplinaire **HAL**, est destinée au dépôt et à la diffusion de documents scientifiques de niveau recherche, publiés ou non, émanant des établissements d'enseignement et de recherche français ou étrangers, des laboratoires publics ou privés.

I. Queinnec, S. Tarbouriech
(LAAS-CNRS, Université de Toulouse, CNRS)

J.-M. Biannic
(ONERA)

C. Prieur
(Univ. Grenoble Alpes, CNRS, Gipsa-lab)

E-mail: queinnec@laas.fr

DOI: 10.12762/2017.AL13-07

Anti-Windup Algorithms for Pilot-Induced-Oscillation Alleviation

The paper deals with the development of anti-windup schemes and related numerical oriented tools. The objective is then to design anti-windup compensators to guarantee stability and performance for some particular classes of nonlinear actuators presenting both magnitude and rate saturations. The lateral flying case for a civil aircraft undergoing aggressive maneuvering by the pilot is addressed. A complete methodology including theoretical conditions and associated toolbox is then proposed and compared to solutions based on anti-PIO filters.

Introduction

The paper is aimed at developing anti-windup schemes and related numerical tools, in order to alleviate the Pilot-Induced-Oscillations in the lateral flying case for a civil aircraft undergoing aggressive maneuvering by the pilot. Indeed, anti-windup strategies represent an appropriate framework to mitigate the undesired saturation effects [24], [31]. Thus, the general principle of the anti-windup scheme can be depicted in Figure 1, where the (unconstrained) signal produced by the controller is compared to what is actually fed into the plant (the constrained signal). This difference is then used to adjust the control strategy by preserving stability and performance.

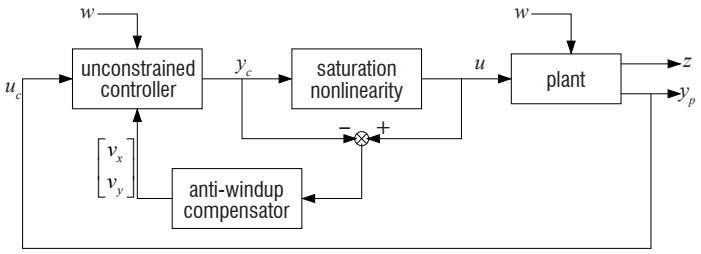


Figure 1 – Anti-windup principle

Such an anti-windup scheme is crucial for many control plants, since adding such a compensator to a previously computed control loop enables the performance of the closed-loop system to be improved, and could even prevent dramatic behavior, such as diverging solutions, when starting from bad initial conditions. For instance, [2], [3], [13], [14], [11], [12], [24] discuss several examples of open-loop unstable or stable physical systems presenting diverging solutions due to the presence of saturations. In particular, this undesirable nonlinear behavior appears for all exponentially unstable open-loop control systems, as well as for some marginally stable open-loop systems, as established in [23], [29].

Actually, this problem is particularly crucial for the space and aeronautical fields, where the Pilot-Induced-Oscillation (PIO) phenomenon is observed; that is, the existence of a particular external excitation (signal w in the notation of Figure 1) renders the closed-loop system unstable without anti-windup compensator [1], [15]. Thus, *ad-hoc* [22], [16] or advanced anti-windup strategies [8], [9], [18] for PIO suppression have been proposed in the literature and applied in practice.

For a given plant in closed loop with a pre-designed controller (designed without taking into account the saturation constraint) and a saturating input, the design of the anti-windup compensator is usually split into two steps, as explained in [26]. First, an analysis study is performed to estimate the effect of the isolated nonlinearity on the performance of the closed-loop system. Then, the second step is the design of an anti-windup compensator to improve the performance. By "performance", various notions could be considered, such as the $\mathcal{L}_2$ gain between a perturbation w and the regulated output z, as depicted in Figure 1. Of course, this performance estimation is associated with an estimation of the region where the initial conditions need to be restricted, in order to guarantee the asymptotic or exponential stability of the origin.

Numerous methods exist for the design of anti-windup compensators for control systems in the presence of magnitude or rate saturation constraints. See, for example, [11], [30], [10], [28], [24], [31] to cite just a few books, surveys or special issues on this subject. Of course, the aim of this paper is not to give an exhaustive perspective about anti-windup compensator design, but rather to present some hints and algorithms on how to solve numerically the anti-windup compensator design problem for an application purpose. Actually, due to the classical tradeoff between performance and estimation of the suitable region of initial conditions, the design of anti-windup

compensators is cast into a static optimization problem, written in terms of Linear Matrix Inequalities (LMIs). Such an optimization problem can be solved numerically in an efficient way using classical software in a Matlab environment. To illustrate the approach and algorithms, the anti-windup compensator design methods are applied to a lateral aircraft model, in order to provide a systematic way to mitigate the PIO phenomenon. Although actuator loss is not exactly the subject of the paper, we illustrate the case where only one aileron is available, allowing us to consider a harsh limit on the actuator bounds to better exhibit the effect of saturation and anti-windup actions.

This paper is organized as follows. First, the model and the problem under consideration are stated in Section "Model description and problem formulation". The main results are presented in Section "Main anti-windup design conditions", where numerically tractable conditions are given to solve the anti-windup compensator design problem and some efficient algorithms are given. The numerical tools used to actually solve the problem are focused on in Section "Dedicated software tools for solving saturated and anti-windup problems". These tools are then illustrated through an application to a realistic model for a civil transport aircraft in Section "PIO alleviation using an anti-windup loop". Some concluding remarks and perspectives end the paper.

Model description and problem formulation

The full model, including the plant, actuator, controller and anti-windup loop, is precisely defined below.

Plant model

We assume that the output of the controller is not affected in a same way by the nonlinear elements. The vector $u \in \Re^m$ building the m inputs of the plant is broken down into two subvectors: the first one, denoted by $u_s \in \Re^{m_s}$, corresponds to m_s saturated inputs, whereas the second one, denoted by $u_{ns} \in \Re^{m-m_s}$, corresponds to the linear inputs (unsaturated inputs). The plant model can be defined by:

$$\text{sysP}: \begin{cases} \dot{x}_p &= A_p x_p + B_{pu}^s u_s + B_{pu}^{ns} u_{ns} + B_{pw} w \\ y_p &= C_p x_p + D_{pu}^s u_s + D_{pu}^{ns} u_{ns} + D_{pw} w \\ z &= C_z x_p + D_{zu}^s u_s + D_{zu}^{ns} u_{ns} + D_{zw} w \end{cases} \quad (1)$$

where $x_p \in \Re^{n_p}$ and $w \in \Re^q$ are the state and the measured output of the plant. $w \in \Re^q$ generally represents an exogenous perturbation, but may also be used to represent a reference signal (or both). Furthermore, $z \in \Re^l$ represents the regulated output, which is used to evaluate the performance of the system with respect to the perturbation w via some appropriate optimization criteria.

Controller model

Unlike the classical anti-windup loops, in which the output of the anti-windup controller is injected into the dynamics of the controller and/or the output of the controller, we consider here that the output of the anti-windup controller modifies only partially the dynamics of the controller and/or the output of the controller. Thus, the dynamical controller is described as follows:

$$\text{sysC}: \begin{cases} \dot{x}_c &= A_c x_c + B_c u_c + B_{cw} w + B_{ca} v_x \\ y_{cs} &= C_c^s x_c + D_c^s u_c + D_{cw}^s w + D_{ca} v_y \\ y_{cns} &= C_c^{ns} x_c + D_c^{ns} u_c + D_{cw}^{ns} w \end{cases} \quad (2)$$

where $x_c \in \Re^{n_c}$ and $u_c \in \Re^p$ are the state and the input of the controller. The output of the controller is broken down into two signals: $y_{cs} \in \Re^{m_s}$, which will be interconnected u_s through a saturated actuator, and $y_{cns} \in \Re^{m-m_s}$, which will be interconnected with the linear (unsaturated) input u_{ns}. Moreover, v_x and v_y are the additional inputs that will be connected to the anti-windup controller. B_{ca} and D_{ca} are matrices of dimensions $n_c \times n_{cr}$ and $m_s \times m_r$, and make it possible to specify what the n_{cr} states and m_r outputs modified by the anti-windup action are.

Actuator model

The actuator block between the output of the controller y_c and the input of the plant u is divided into two blocks: the first one corresponding to the nonlinear (saturated) part and the second one corresponding to the linear (unsaturated) part. The nonlinear actuator part involves n_{dz} nested saturations, including the case of rate and magnitude saturations, as depicted in Figure 2(a). Such nonlinearities are tackled via the use of dead-zone, denoted by $\phi_i(.)$, $i = 1,...,n_{dz}$.

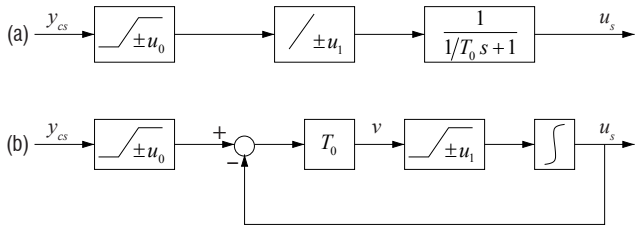


Figure 2 – (a) Actuator with rate and magnitude saturations. (b) Model used to represent such an actuator (scalar case)

The dynamical model of the actuator is based on Scheme 2(b) as follows:

$$\text{with} \quad sysACT: \begin{cases} \dot{x}_a &= v + \phi_1(v) \\ v &= T_0 y_{cs} + T_0 \phi_0(y_{cs}) - T_0 x_a \\ u_s &= x_a \end{cases} \quad (3)$$

where $\phi_0(y_{cs}) = sat_{u_0}(y_{cs}) - y_{cs}$ and $\phi_1(v) = sat_{u_1}(v) - v$. $sat_{u_0}(.)$ and $sat_{u_1}(.)$ are classical saturation functions and u_0 and u_1 are the levels of saturation in magnitude and rate, respectively. The elements of the diagonal matrix $T_0 \in \Re^{m_s \times m_s}$ classically take on large enough values, in order to avoid affecting the linear dynamics of the closed-loop system.

Anti-windup compensator

In the DLAW (Direct Linear Anti-Windup) strategy, the anti-windup controller uses as input the difference between the signals issued either from the input and the output of the whole actuator or from the input and the output of the nonlinear elements included in the actuator. Then, the anti-windup loop under consideration in the paper considers that the inputs of the anti-windup controller are the dead-zones associated with each saturation. Hence, the anti-windup controller of order n_{aw} is written as:

$$AW_\phi: \begin{cases} \dot{x}_{aw} &= A_{aw} x_{aw} + B_{aw}^0 \phi_0(y_c) + B_{aw}^1 \phi_1(v) \\ \begin{bmatrix} v_x \\ v_y \end{bmatrix} &= C_{aw} x_{aw} + D_{aw}^0 \phi_0(y_c) + D_{aw}^1 \phi_1(v) \end{cases} \quad (4)$$

where v_x and v_y are of dimensions n_{cr} and m_r, respectively.

Interconnections

The interconnections considered can be described as follows:

- linear link between the output of the plant and the input of the controller: $u_c = y_p$;

- the first part of the output of the controller (y_{cs}) is linked to the corresponding inputs of the plant (u_s) through the actuator model (3);
- the second part of the output of the controller is directly connected to the corresponding inputs of the plant: $u_{ns} = y_{cns}$;
- v_x and v_y are built from the anti-windup compensator.

Remark 2.1

An important fact is that the anti-windup model (4) imposes the assumption that the input and output signals of each saturation block in Figure 2 are available. To overcome this assumption, alternative strategies can be investigated. For example, the anti-windup may use the difference between the nonlinear actuator and a linear fictitious one (with the same dynamics but without saturation blocks) to explicitly take into account the dynamics of the actuator (present in the rate limiter) [20]. Another option would be to build an observer to evaluate the internal state of the actuator [27].

Standard formulation

In [24], a standard formulation of the anti-windup design has been proposed for various kinds of actuators. In the current case, by considering an augmented state of dimensions $n = n_p + m_s + n_c + n_{aw}$ including the state of the plant, the state of the actuator, the state of the controller and the state of the anti-windup controller, the following standard model of the complete closed-loop system can be defined by:

$$\begin{cases} \dot{x} &= \mathcal{A}x + \mathcal{B}_0\phi_0(y_c) + \mathcal{B}_1\phi_1(v) + \mathcal{B}_2 w \\ y_c &= \mathcal{C}_0 x + \mathcal{D}_{00}\phi_0(y_c) + \mathcal{D}_{01}\phi_1(v) + \mathcal{D}_{0w} w \\ v &= \mathcal{C}_1 x + \mathcal{D}_{10}\phi_0(y_c) + \mathcal{D}_{11}\phi_1(v) + \mathcal{D}_{1w} w \\ z &= \mathcal{C}_2 x + \mathcal{D}_{20}\phi_0(y_c) + \mathcal{D}_{21}\phi_1(v) + \mathcal{D}_{2w} w \end{cases} \quad (5)$$

where the matrices of the anti-windup controller are encapsulated into the matrices of system (5). Details of these matrices are given in Section "Algorithms for AW_ϕ design".

The design procedure of the anti-windup controller consists in optimizing some quantities, such as the size of the region of stability of the closed-loop system or the guaranteed level of performance. In particular, the idea when adding the anti-windup loop is to maximize the basin of attraction of the origin for the closed-loop system and/or to minimize the $\mathcal{L}_2$ gain between w and z or to maximize the set of perturbation w, which can be rejected. Then, the perturbation signal is assumed to be bounded in energy, as follows:

$$\|w\|_2^2 = \int_0^\infty w'(t)w(t)dt \le \delta^{-1};\ 0 \le \delta^{-1} < \infty \quad (6)$$

The problem that we intend to address is summarized below.

Problem 2.2

Determine an anti-windup controller AW_ϕ and a region $\mathcal{E}$, as large as possible, such that

- *Internal stability. When $w = 0$, the closed-loop system (5) is asymptotically stable for any initial conditions belonging to $\mathcal{E}$ (which is a region of asymptotic stability (RAS));*
- *Performance. When $w \neq 0$, satisfying (6), and for $x(0) = 0$, the $\mathcal{L}_2$ gain between w and z is finite and equal to $\gamma > 0$. Furthermore, the trajectories of the closed-loop system (5) remain bounded in the set $\mathcal{E}$.*

The convex optimization problems associated with Problem 2.2 are specified in Section "Algorithms for AW_ϕ design".

Main anti-windup design conditions

Solution to standard anti-windup design

The following proposition provides conditions of local stability and $\mathcal{L}_2$ performance for the closed-loop system (5). The result considers existence conditions to solve Problem 2.2.

Proposition 3.1

If there exist a symmetric positive definite matrix $Q \in \Re^{n\times n}$, two matrices Z_0 and $Z_1 \in \Re^{m\times n}$, two positive diagonal matrices S_0 and $S_1 \in \Re^{m\times m}$ and a positive scalar γ such that the following conditions are met:

$$\begin{bmatrix} Q\mathcal{A}' + \mathcal{A}Q & \mathcal{B}_0S_0 - Q\mathcal{C}_0' - Z_0' & \mathcal{B}_1S_1 - Q\mathcal{C}_1' - Z_1' & \mathcal{B}_2 & Q\mathcal{C}_2' \\ \star & -2S_0 - \mathcal{D}_{00}S_0 - S_0\mathcal{D}_{00}' & -\mathcal{D}_{01}S_1 - S_0\mathcal{D}_{10}' & -\mathcal{D}_{0w} & S_0\mathcal{D}_{20}' \\ \star & \star & -2S_1 - \mathcal{D}_{11}S_1 - S_1\mathcal{D}_{11}' & -\mathcal{D}_{1w} & S_1\mathcal{D}_{21}' \\ \star & \star & \star & -I & \mathcal{D}_{2w}' \\ \star & \star & \star & \star & -\gamma I \end{bmatrix} < 0 \quad (7)$$

$$\begin{bmatrix} Q & Z_{0(i)}' \\ \star & \delta u_{0(i)}^2 \end{bmatrix} \ge 0,\ i = 1,\ldots,m \quad (8)$$

$$\begin{bmatrix} Q & Z_{1(i)}' \\ \star & \delta u_{1(i)}^2 \end{bmatrix} \ge 0, i = 1,\ldots,m \quad (9)$$

then,

1. *when $w = 0$, the set $E(Q^{-1},\delta) = \{x \in \Re^n; x'Q^{-1}x \le \delta^{-1}\}$ is RAS for the closed-loop system (5);*
2. *when $x(0) = 0$, satisfying (6), and for $x(0) = 0$,*
   - *the trajectories of the closed-loop system remain bounded in the set $\mathcal{E}(Q^{-1},\delta)$;*
   - *the $\mathcal{L}_2$ gain is finite and one obtains:*

$$\int_0^T z(t)'\,z(t)dt \le \gamma \int_0^T w(t)'\,w(t)dt,\ \forall T \ge 0 \quad (10)$$

The detailed way to derive the conditions and to prove them can be found, for example, in [24], [31].

Remark 3.2

The interest of the anti-windup structure resides in the simplicity of the design conditions. Indeed, the design of a static anti-windup gain (only matrices D_{aw}^0 and D_{aw}^1 are used) is the result of a fully linear problem. In the case of the design of a dynamical anti-windup controller, for a priori given matrices A_{aw} and C_{aw}, the determination of the input and transmission matrices is also obtained by solving a linear problem. In the case where $n_{aw} = n_p + n_{m_s} + n_c$, the resolution of a linear problem can also be considered through an iterative procedure [24].

For analysis purposes (the anti-windup controller being given), the conditions of Proposition 3.1 are linear and can be directly used to solve adequate optimization problems. Moreover, in the design context, the conditions of Proposition 3.1 are non-convex, matrices A_{aw}, B_{aw}, C_{aw} and D_{aw}, hidden in matrices $\mathcal{A}$, $\mathcal{B}_i$, $\mathcal{C}_i$, $\mathcal{D}_{ij}$, $i,j = 0,1$. Conditions with linear decision variables can be obtained, more or less directly, by slightly modifying the original conditions, or even by considering iterative procedures (including D-K iteration process)

allowing a Lyapunov matrix and anti-windup matrices to be sought. These situations are detailed in the next subsection.

Remark 3.3

In the sequel, one considers a set $\mathcal{X}_0$, defined by some directions in the plant state space $v_i \in \Re^{n_p}$, $i = 1,...,q$, to provide a desired shape of the region $E(Q^{-1},\delta)$ to be maximized when solving Problem 2.2. Then, considering $\overline{v}_i = \begin{bmatrix} v_i' & 0 \end{bmatrix}' \in \Re^n$, $i = 1,...,q$ and β a scaling factor such that $\beta\overline{v}_i \in E(Q^{-1},\delta)$, $i = 1,...,q$ (which corresponds to imposing $\beta\mathcal{X}_0 \subset E(Q^{-1},\delta)$), an additional condition to those of Proposition 3.1 must be considered in the algorithms, as follows:

$$\begin{bmatrix} \delta\dfrac{1}{\beta^2} & \delta\overline{v}_i' \\ \delta\overline{v}_i & Q \end{bmatrix} > 0,\ i = 1,...,q \tag{11}$$

This means that β is used to maximize the region of attraction of the system and $\mathcal{X}_0$ allows the directions of interest for this region of attraction to be oriented.

Algorithms for AW_ϕ design

From (1), (2), (3) and (4), the matrices of system (5) are defined by:

$$\begin{gathered}
\mathcal{A} = \begin{bmatrix} \mathbb{A} & B_v C_{aw} \\ 0 & A_{aw} \end{bmatrix} \qquad \mathcal{B}_0 = \begin{bmatrix} B_{\phi 0} + B_v D_{aw}^0 \\ B_{aw}^0 \end{bmatrix} \qquad \mathcal{B}_1 = \begin{bmatrix} B_{\phi 1} + B_v D_{aw}^1 \\ B_{aw}^1 \end{bmatrix} \\
\mathcal{C}_0 = \begin{bmatrix} C_0 & C_{v0} C_{aw} \end{bmatrix} \qquad \mathcal{C}_1 = \begin{bmatrix} C_1 & C_{v1} C_{aw} \end{bmatrix} \qquad \mathcal{C}_2 = \begin{bmatrix} C_2 & 0 \end{bmatrix} \\
\mathcal{D}_{00} = C_{v0} D_{aw}^0 \qquad \mathcal{D}_{01} = C_{v0} D_{aw}^1 \qquad \mathcal{D}_{10} = D_1 + C_{v1} D_{aw}^0 \qquad \mathcal{D}_{11} = C_{v1} D_{aw}^1 \\
\mathcal{B}_2 = \begin{bmatrix} B_2 \\ 0 \end{bmatrix} \qquad \mathcal{D}_{20} = 0 \qquad \mathcal{D}_{21} = 0
\end{gathered} \tag{12}$$

with

$$\mathbb{A} = \begin{bmatrix} A_p + B_{pu}^{ns}\Delta^{-1} D_c^{ns} C_p & B_{pu}^s + B_{pu}^{ns}\Delta^{-1} D_c^{ns} D_{pu}^s & B_{pu}^{ns}\Delta^{-1} C_c^{ns} \\ T_0 D_c^s \left(C_p + D_{pu}^{ns}\Delta^{-1} D_c^{ns} C_p\right) & T_0\left(D_c^s D_{pu}^s - I_{ms} + D_c^s D_{pu}^{ns}\Delta^{-1} D_c^{ns} D_{pu}^s\right) & T_0\left(C_c^s + D_c^s D_{pu}^{ns}\Delta^{-1} C_c^{ns}\right) \\ B_c C_p + B_c D_{pu}^{ns}\Delta^{-1} D_c^{ns} C_p & B_c D_{pu}^s + B_c D_{pu}^{ns}\Delta^{-1} D_c^{ns} D_{pu}^s & A_c + B_c D_{pu}^{ns}\Delta^{-1} C_c^{ns} \end{bmatrix}$$

$$B_2 = \begin{bmatrix} B_{pw} + B_{pu}^{ns}\Delta^{-1}\left(D_c^{ns} D_{pw} + D_{cw}^{ns}\right) \\ T_0\left(D_c^s D_{pw} + D_{cw}^s + D_c^s D_{pu}^{ns}\Delta^{-1}\left(D_c^{ns} D_{pw} + D_{cw}^{ns}\right)\right) \\ B_{cw} + B_c D_{pw} + B_c D_{pu}^{ns}\Delta^{-1}\left(D_c^{ns} D_{pw} + D_{cw}^{ns}\right) \end{bmatrix}$$

$$B_{\phi 0} = \begin{bmatrix} 0 \\ T_0 \\ 0 \end{bmatrix} \qquad B_{\phi 1} = \begin{bmatrix} 0 \\ I_{m_s} \\ 0 \end{bmatrix} \qquad D_1 = T_0$$

$$\begin{aligned}
C_0 &= \begin{bmatrix} D_c^s\left(I_p + D_{pu}^{ns}\Delta^{-1} D_c^{ns}\right) C_p & D_c^s\left(I_p + D_{pu}^{ns}\Delta^{-1} D_c^{ns}\right) D_{pu}^s & C_c^s + D_c^s D_{pu}^{ns}\Delta^{-1} C_c^{ns} \end{bmatrix} \\
C_1 &= \begin{bmatrix} T_0 D_c^s\left(I_p + D_{pu}^{ns}\Delta^{-1} D_c^{ns}\right) C_p & T_0 D_c^s\left(I_p + D_{pu}^{ns}\Delta^{-1} D_c^{ns}\right) D_{pu}^s - T_0 T_0\left(C_c^s + D_c^s D_{pu}^{ns}\Delta^{-1} C_c^{ns}\right) \end{bmatrix} \\
C_2 &= \begin{bmatrix} C_z + D_{zu}^{ns}\Delta^{-1} D_c^{ns} C_p & D_{zu}^s + D_{zu}^{ns}\Delta^{-1} D_c^{ns} D_{pu}^s & D_{zu}^{ns}\Delta^{-1} C_c^{ns} \end{bmatrix}
\end{aligned}$$

$$\begin{aligned}
D_{0w} &= D_{cw}^s + D_c^s D_{pw} + D_c^s D_{pu}^{ns}\Delta^{-1}\left(D_c^{ns} D_{pw} + D_{cw}^{ns}\right) \\
D_{1w} &= T_0\left(D_{cw}^s + D_c^s D_{pw} + D_c^s D_{pu}^{ns}\Delta^{-1}\left(D_c^{ns} D_{pw} + D_{cw}^{ns}\right)\right) \\
D_{2w} &= D_{zw} + D_{zu}^{ns}\Delta^{-1}\left(D_c^{ns} D_{pw} + D_{cw}^{ns}\right)
\end{aligned}$$

Furthermore, matrices defining the interconnection between the anti-windup loop and the system are:

$$B_v = \begin{bmatrix} 0 \\ T_0 D_{ca}\begin{bmatrix} 0 & I_{m_r} \end{bmatrix} \\ B_{ca}\begin{bmatrix} I_{n_{cr}} & 0 \end{bmatrix} \end{bmatrix} \qquad C_{v0} = D_{ca}\begin{bmatrix} 0 & I_{m_r} \end{bmatrix} \qquad C_{v1} = T_0 D_{ca}\begin{bmatrix} 0 & I_{m_r} \end{bmatrix}$$

The analysis problem (Algorithm 3.4) is linear and the synthesis problem of the anti-windup is nonlinear, including products between decision variables and, in particular, between the Lyapunov matrix Q and the anti-windup elements. A D-K iteration procedure may then be considered for the synthesis problem (Algorithm 3.6). However, the synthesis optimization problem may be partially linearized and, for given matrices A_{aw} and C_{aw}, the design of matrices B_{aw}^i and D_{aw}^i, $i = 0,1$ can be handled via a linear optimization problem (Algorithm 3.5).

Algorithm 3.4

Analysis of a given AW_ϕ anti-windup controller

1. *Select matrices A_{aw}, B_{aw}^0, B_{aw}^1, D_{aw}^0, D_{aw}^0 and D_{aw}^1.*
2. *Choose directions to be optimized $v_i \in \Re^{n_p}$, $i = 1,...,q$ and a known perturbation bound δ.*
3. *Solve*

$$\min_{Q, S_0, S_1, Z_0, Z_1, \gamma, \mu} f_{cost}(\gamma, \mu)$$

subject to LMI (7), (8), (9) *and* (11)

where γ is the $\mathcal{L}_2$ gain between w and z and $\mu = 1/\beta^2$.

Algorithm 3.5

Design of an AW_ϕ anti-windup controller with fixed dynamics

1. *Select matrices A_{aw} and C_{aw}. A static anti-windup AW_ϕ may also be used by considering $n_{aw} = 0$.*
2. *Choose directions to be optimized $v_i \in \Re^{n_p}$, $i = 1,...,q$ and a known perturbation bound δ.*
3. *Solve*

$$\min_{Q, S_0, S_1, Z_0, Z_1, \bar{B}_{aw}^0, \bar{B}_{aw}^1, \bar{D}_{aw}^0, \bar{D}_{aw}^1, \gamma, \mu} f_{cost}(\gamma, \mu)$$

subject to LMI (7), (8), (9) *and* (11)

where γ is the $\mathcal{L}_2$ gain between w and z and $\mu = 1/\beta^2$.

4. *Compute $B_{aw}^0 = \bar{B}_{aw}^0 S_0^{-1}$, $B_{aw}^1 = \bar{B}_{aw}^1 S_1^{-1}$, $D_{aw}^0 = \bar{D}_{aw}^0 S_0^{-1}$ and $D_{aw}^1 = \bar{D}_{aw}^1 S_1^{-1}$.*

Algorithm 3.6

Design of an AW_ϕ anti-windup controller – full design

1. *Select matrices A_{aw}, C_{aw} of appropriate dimensions, in order to build the desired anti-windup loop.*
2. *Choose the directions to be optimized $v_i \in \Re^{n_p}$, $i = 1,...,q$ and a known perturbation bound δ.*
3. *Pre-synthesis step – Solve*

$$\min_{Q, S_0, S_1, Z_0, Z_1, \bar{B}_{aw}^0, \bar{B}_{aw}^1, \bar{D}_{aw}^0, \bar{D}_{aw}^1, \gamma, \mu} f_{cost}(\gamma, \mu)$$

subject to LMI (7), (8), (9) *and* (11)

where γ is the $\mathcal{L}_2$ gain between w and z and $\mu = 1/\beta^2$.

4. *Compute $B_{aw}^1 = \bar{B}_{aw}^1 S_1^{-1}$, $B_{aw}^1 = \bar{B}_{aw}^1 S_1^{-1}$, $D_{aw}^0 = \bar{D}_{aw}^0 S_0^{-1}$ and $D_{aw}^1 = \bar{D}_{aw}^1 S_1^{-1}$.*
5. *If the solution obtained is satisfactory (some accuracy has to be fixed), or no longer improved compared to the previous steps, then STOP. Otherwise, go to the next iteration (the idea is to finish by a pre-synthesis step).*
6. *Synthesis step – Pick the solution Q obtained at Step 3 and solve*

$$\min_{S_0, S_1, Z_0, Z_1, A_{aw}, C_{aw}, B_{aw}^0, B_{aw}^1, D_{aw}^0, D_{aw}^1, \gamma} \gamma$$

subject to LMI (7), (8), (9) *and* (11)

7. Go to Step 3.

Remark 3.7

The optimization cost function f_{cost} is typically related to the performance of the disturbance rejection ($min\ \gamma$) and/or to the size of the domain of safe behavior in which the trajectories of the system may be initiated. In this paper, we consider inequalities (11) and $min\ \mu$, with $\mu = 1/\beta^2$ but any other criterion of the matrix B_{aw}^i could be used.

Remark 3.8

In Algorithm 3.5 and in Step 3 of Algorithm 3.6, condition (7) is not directly applied. The products between B_{aw}^i and D_{aw}^i with the matrices S_i are replaced by the change of variables $\bar{B}_{aw}^i$ and $\bar{D}_{aw}^i$, $i = 0,1$, which allows the problem to be linearized.

Remark 3.9

An interesting case is the static anti-windup one, for which matrices A_{aw} and C_{aw} are null matrices of appropriate dimensions. It implies that B_{aw}^i, $i = 0,1$, are also null matrices of appropriate dimensions and only matrices D_{aw}^i, $i = 0,1$, are computed in Algorithm 3.5.

Remark 3.10

Matrices A_{aw} and C_{aw} to be used in Algorithm 3.5 may be selected as the solution to a full-order ($n_{aw} = n_p + n_c + m_s$) anti-windup compensator design where the actuator is just a saturation in magnitude (see, for example, the conditions provided in [24]), i.e., *via a linear optimization problem. Eventually, an order-reduction step may also be considered in order to select matrices A_{aw} and C_{aw} (see Example 8.5 in [24]). Other procedures developed in [31], such as the Model Recovery Anti-Windup (MRAW), could be used.*

Dedicated software tools for solving saturated and anti-windup problems

For numerical evaluations, Semi-Definite Programming (SDP) solvers are easily available in a Matlab environment, either considering the MathWorks® package LMI Lab included in the Robust Control Toolbox™ or any freely available solvers. Similarly, in addition to the original parser of the LMI Lab package, one may prefer YALMIP format [17] to specify LMIs systems, convex optimization costs and associated solvers.

SATAW toolbox [19] has been developed to perform analysis and control design operations for linear systems interconnected with saturation elements. The toolbox manipulates a flexible description of the continuous-time system, controller and actuator using simple structure elements, as they are described in Section "Main anti-windup design conditions". For the saturation modeling, sector conditions are used. In this representation, the saturation term is replaced by a dead-zone nonlinearity. Hence, sector conditions, locally or globally valid, can be used to provide stability and stabilization conditions. The package then includes several functions for:

- state feedback or output feedback analysis, in the presence of position saturation and/or rate saturation;
- state feedback or output feedback design, in the presence of position saturation;
- static and dynamic anti-windup analysis, in the presence of position saturation;
- static anti-windup design, in the presence of position saturation.

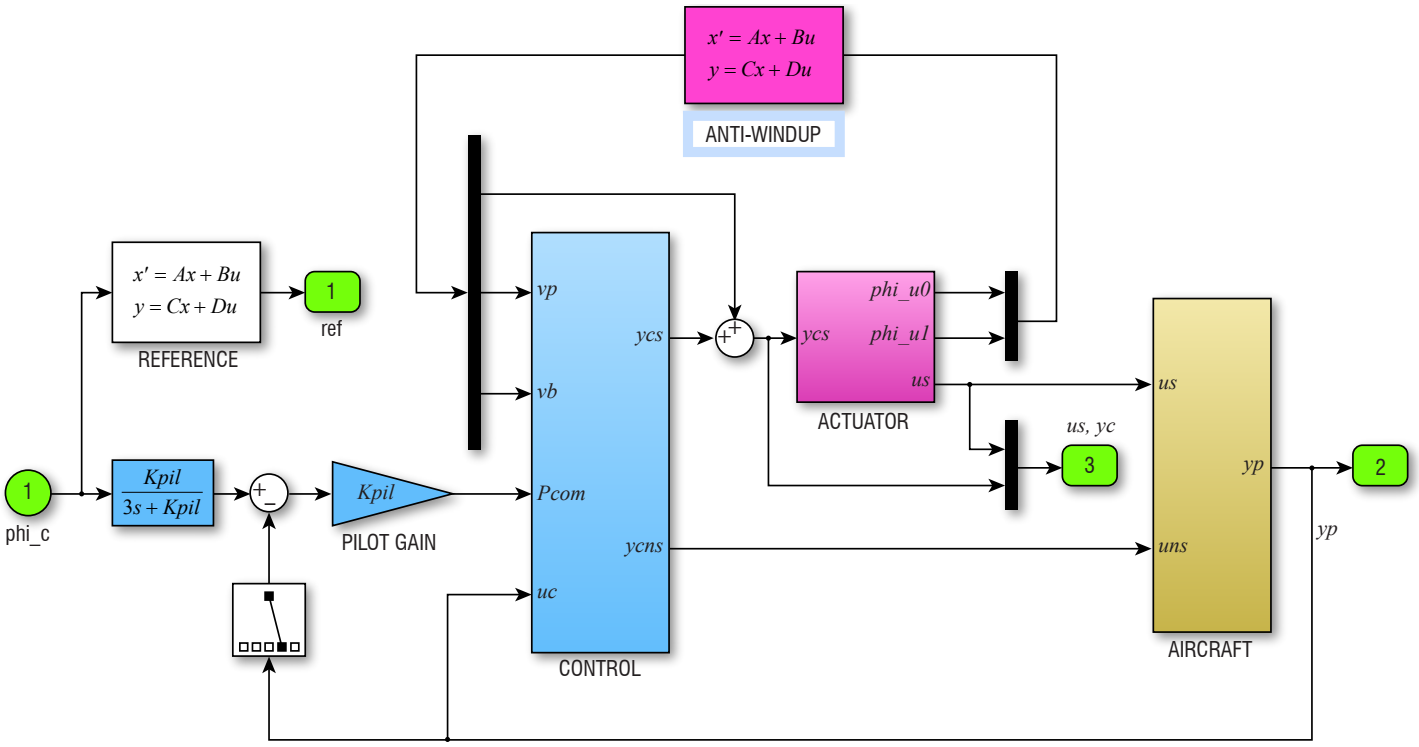


Figure 3 – Nonlinear closed-loop Simulink implementation of anti-windup AW_ϕ for lateral aircraft simulations

Actually, the current published version of the toolbox does not allow the dynamic anti-windup design problem to be formally solved in the presence of position and rate saturation, but gives many elements to extend the functions to the case addressed in this paper.

Alternatively, the AWAST Tools [5], which were recently updated and integrated as a library (SAW Library) of the SMAC Toolbox [4], enable rather general anti-windup problems to be formalized and solved, following the practical framework proposed in [6].

PIO alleviation using an anti-windup loop

The design and analysis algorithms of Section "Main anti-windup design conditions" are now applied and compared in the realistic context of lateral maneuvers of a civil transport aircraft. Specific attention is devoted to aggressive pilot demands in conjunction with actuator loss.

To do this, the pilot's activity is modeled as a static gain K_{pil}. For this application, a normal activity would correspond to $K_{pil} = 1$. Actually, in stressful situations, notably in case of actuator loss, a more aggressive pilot behavior is generally observed, resulting in much higher gains. Here, the gain is set to $K_{pil} = 2$.

Problem setup and objectives

A nonlinear closed-loop Simulink implementation of the anti-windup structure is depicted in Figure 3. The "aircraft" block is a linearized version (for fixed airspeed and altitude under cruise flight conditions) of the lateral dynamics of the system, including structural filters and delays, resulting in a state-space model of dimension 63. The controller block includes a dynamical controller of dimension 29. Its central objective is to provide good damping for the Dutch roll and to enable a safe control of the roll rate so that the bank angle ϕ is then easily controlled by the pilot with a simple gain K_{pil}. The state-space models $sysP$ and $sysC$ are then readily obtained from the Simulink diagrams of Figure 3, with the help of the Matlab **linmod** function. The plant corresponds to the "yellow box" depicting the aircraft system while the global controller (including pilot actions) is obtained by extraction of the 3 blue boxes. A standard balanced reduction technique is finally applied to obtain reasonably sized models. The reduced orders obtained, respectively $n_p = 8$ and $n_c = 20$, are compatible with the proposed algorithms.

The aircraft system involves 2 control inputs ($m = 2$): ailerons and rudder deflections. Note that only the aileron deflection actuator is assumed to saturate ($m_s = 1$) for the considered maneuvers. Moreover, 5 outputs ($p = 5$) are available for feedback ($y_p = [\beta, p, r, \phi, \dot{\phi}]'$). The performance is evaluated via the tracking accuracy on the fourth bank-angle output ϕ (then, $l = 1$). The disturbance input of System (1) is used to express the perturbing effect of the saturation of the system input, that is, $B_{pw} = B^s_{pu}$ ($q = 1$).

In the AW_ϕ strategy, two signals (one for the magnitude limitation and one for the rate limitation) are used by the anti-windup device. Their generation is detailed in the Simulink implementation of Figure 4.

The anti-windup controller acts on the internal dynamics of the nominal lateral controller of the aircraft through two scalar signals v_p and v_b, which respectively affect roll and sideslip angle dynamics ($v_x = [v_p \;\; v_b]$ and $v_y = 0$, $n_{cr}=2$, $m_r = 0$). This means that matrix B_{ca} appearing in Equation (2) is of dimension $n_c \times 2$.

The chosen strategy offers some flexibility, with the possibility of a direct anti-windup action at the controller output. However, no significant improvement has been observed with this additional feature, which has thus not been further considered in this application. This means that D_{ca} appearing in Equation (2) is equal to 0.

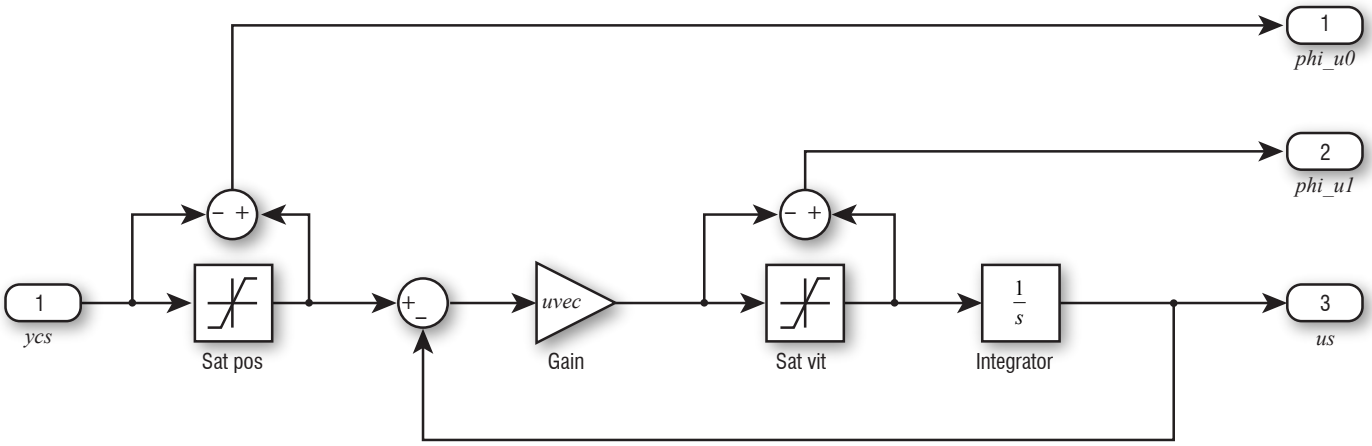


Figure 4 – Detailed view of the magnitude and rate limitation system

The main objective of this application is to design and evaluate anti-windup compensators to improve the aircraft response to roll angle solicitations while limiting oscillations despite actuator loss [18]. During such maneuvers, a significant control activity is observed on the ailerons. This is why the effects of saturations are modeled and taken into account for these actuators in the diagram of Figure 3, while no saturation is introduced on the rudders. The effects of saturations become even more penalizing in case of a partial loss of control capability. Assume indeed that the aircraft is controlled by a pair of ailerons on each wing, but that only one is operational. In that case, the activity of the remaining actuators is doubled, as well as the risk of magnitude and rate saturations. Then, the magnitude and rate limits in the following are halved. We consider $u_0 = L_m = 10$ deg (instead of 20 under normal conditions) and $u_1 = L_r = 20$ deg (instead of 40).

In the following, various cases studies are implemented and compared:

- Unsaturated – A non-saturated case where saturation elements are removed allows an ideal behavior of the closed-loop system to be exhibited;
- Saturated – A saturated case without compensation strategy is used as the nominal behavior of the closed-loop saturated system;
- Anti-PIO filter – The standard anti-PIO filter used in the industry is an "open-loop" solution that does not exploit the information relative to the saturation of the signal (see [7]). It may be considered as the basic solution from the industry. This strategy consists in adding a dynamical block with pre-saturation between the pilot gain (K_{pil}) and the control block. The full scheme is hidden in the block REFERENCE in Figure 3;
- Static AW_ϕ – A static version of our anti-windup strategy is designed with Algorithm 3.5. This strategy is an alternative to the standard anti-PIO filter, since it is very easy to implement (no additional dynamical system to introduce in the controller block);
- Dynamic AW_ϕ – A dynamic version of our anti-windup is designed with Algorithm 3.5. Various cases initializing the procedures with given matrices A_{aw} and C_{aw} are investigated;
- $\mathcal{H}_\infty AW_e$ – A dynamic anti-windup built using a structured $\mathcal{H}_\infty$ design method [18] is also implemented to compare dynamic anti-windup strategies. The advantage of such a strategy is that it circumvents some limitations of LMI-based strategies (limitation on the problem size when manipulating LMIs, conservatism of sufficient conditions), but to the detriment of ease of construction for engineers who are not always specialists in advanced control theories. Note that, unlike the approach addressed in this paper, the signal used as input for the anti-windup scheme is the difference between the output and the input of the nonlinear block (denoted by e).

In what follows, reduced size models are used for stability analysis and to compute the anti-windup controllers. Full size models of the aircraft and controllers are used for all of the simulations.

Design of a static anti-windup AW_ϕ

Let us first consider the design of a static AW_ϕ anti-windup where only matrices D_{aw}^i, $i = 0,1$ (see Equation (4)), have to be designed ($n_{aw} = 0$). The main advantage is that Condition (7) becomes linear and that the anti-windup block does not involve any additional dynamics. The optimization problem is solved by considering the bound on perturbation $\delta = 0.1$ and $v_1 = \left[C_p(4;:)\,0\right]$, corresponding to the roll angle, as the direction to be optimized over the set $E\left(Q^{-1},\delta\right)$. Algorithm 3.5, followed by Algorithm 3.4, provide the following optimal solution:

Static AW_ϕ design: $\gamma = 1.18110$; $\beta = 0.7808$

with the static anti-windup gains:

$$D_{aw}^0 = \begin{bmatrix} -14.7887 \\ 8.6544 \\ 0 \end{bmatrix} \quad D_{aw}^1 = \begin{bmatrix} -0.0042 \\ 0.0392 \\ 0 \end{bmatrix}$$

which shows that the anti-windup hardly uses the rate saturation information. Moreover, it is interesting to perform the same analysis for the saturated closed-loop system without anti-windup. The feasibility is also obtained and the solution is:

Analysis without anti-widup: $\gamma = 1.8560$; $\beta = 0.7796$

The solution with the static AW_ϕ anti-windup described through γ and β as performance indicators does not appear to be much better than the one without anti-windup: the anti-windup allows γ to be decreased and β to be increased, but only slightly. This does not reflect, however, the simulations described below, which show that the anti-windup action significantly improves the transient behavior of the roll angle, avoiding a large overshoot and degraded time evolution

with respect to the saturated case. The meaning of this is that the considered optimization criterion, which does not explicitly include the time response performance, does not exactly fit the analysis or design of the anti-windup loop. Nevertheless, considering criteria on time response performance is a difficult task and the optimization criterion used here gives a reasonable trade-off between stability guarantee, performance and time response.

Figures 5 and 6 illustrate the time evolution of the closed-loop system to a roll solicitation of 40 deg at time $t = 1$ s followed by a step of –60 deg at time $t = 15$ s and a step of +60 deg at time $t = 30$ s. The responses are compared by considering the case with saturation and no compensation (saturated), a standard anti-PIO strategy (anti-PIO filter) and the static AW_ϕ anti-windup strategy. It is important to underline that a simple static anti-windup strategy enables better performance than the standard anti-PIO case to be obtained, which adds dynamics to the system.

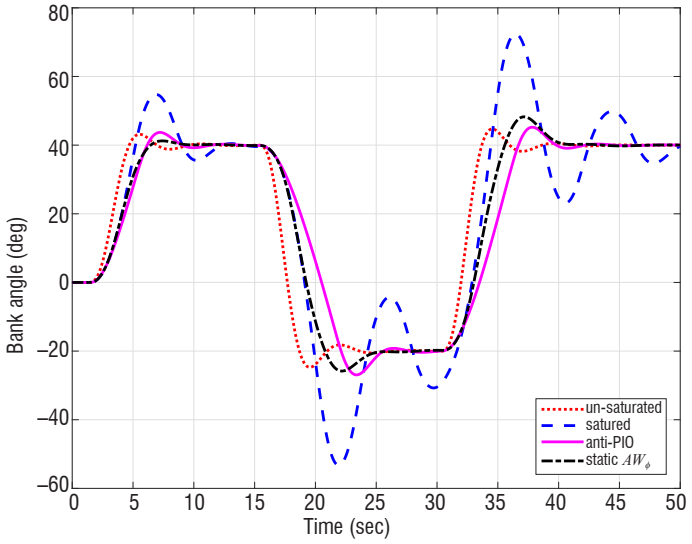


Figure 5 – roll solicitation of +40 deg at time $t = 1$ s followed by a step of –60 deg at time $t = 15$ s and a step of +60 deg at time $t = 30$ s: comparison of the performance output for the un-saturated, saturated (no compensation of the saturation), standard anti-PIO and static anti-windup AW_ϕ simulations

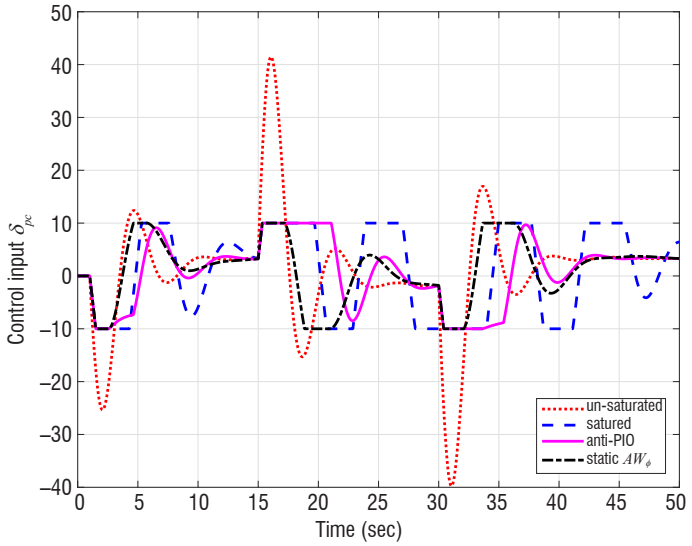


Figure 6 – roll solicitation of +40 deg at time $t = 1$ s followed by a step of –60 deg at time $t = 15$ s and a step of +60 deg at time $t = 30$ s: comparison of the saturating input for the un-saturated, saturated (no compensation of the saturation), standard anti-PIO and static anti-windup AW_ϕ simulations

Design of a dynamic anti-windup AW_ϕ

To go further, let us now consider the design of a dynamic anti-windup AW_ϕ. The difficulty in that case is to initialize the iterative procedure described in Algorithm 3.6, or to select matrices A_{aw} and C_{aw} used in Algorithm 3.5. As for the static case, the optimization problem is solved by considering the bound on perturbation $\delta = 0.1$ and $v_1 = \left[C_p(4;:)\ 0 \right]$ as the direction to be optimized over the set $\varepsilon\left(Q^{-1}, \delta\right)$.

Let us first consider a very simple structure to set matrices A_{aw} and C_{aw}, namely a modal structure for A_{aw} allowing its dynamics to be set slightly faster than those of the closed-loop linear system:

$$A_{aw} = \begin{bmatrix} -100 & 50 \\ -50 & -100 \end{bmatrix} \quad C_{aw} = \begin{bmatrix} -10 & 0 \\ 0 & 10 \\ 0 & 0 \end{bmatrix}$$

Algorithm 3.5 followed by Algorithm 3.4 provides the following optimal solution:

Dynamic AW_ϕ design 1: $\gamma = 1.7863$; $\beta = 0.8334$

with the anti-windup terms:

$$B_{aw}^0 = \begin{bmatrix} 9461.4 \\ -7872.5 \end{bmatrix} \quad B_{aw}^1 = \begin{bmatrix} 60.6 \\ -32.9 \end{bmatrix} \quad D_{aw}^0 = \begin{bmatrix} 438.2 \\ 1009 \\ 0 \end{bmatrix} \quad D_{aw}^1 = \begin{bmatrix} 3.5 \\ 5.1 \\ 0 \end{bmatrix}$$

Another option is to use matrices A_{aw} and C_{aw}, which are the solution to another dynamic anti-windup scheme implemented on the same application. The idea is to circumvent the nonlinear problem of the dynamic anti-windup by pre-selecting matrices A_{aw} and C_{aw} obtained from other approaches, when they exist, with the expectation of obtaining better results than with a "random" selection as done above. In the current case, we consider the solution obtained with a structured $\mathcal{H}_\infty$ design method [18], and previously applied on the same numerical evaluation [7]. In that case, Algorithm 3.5 gives matrices B_{aw}^i and D_{aw}^i, $i = 0,1$, (not provided here for readability reasons) and the following optimal solution:

Dynamical AW_ϕ design 2: $\gamma = 1.7395$; $\beta = 0.9147$

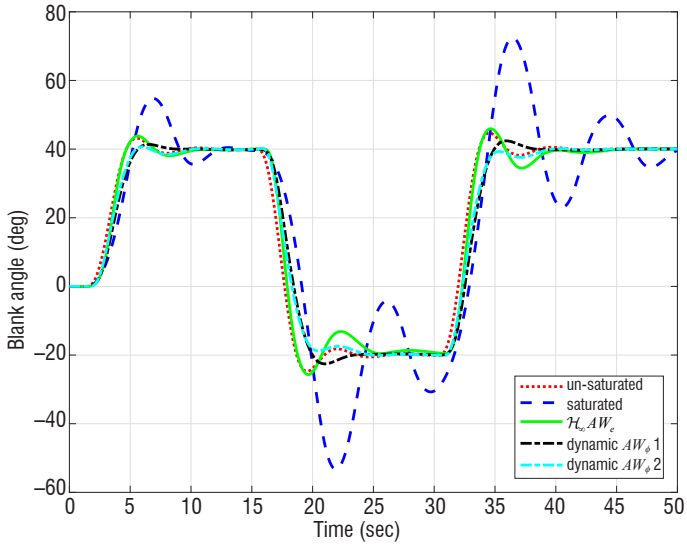


Figure 7 – roll solicitation of +40 deg at time $t = 1$ s followed by a step of –60 deg at time $t = 15$ s and a step of +60 deg at time $t = 30$ s: comparison of the performance outputs for the un-saturated, saturated (no compensation of the saturation), $\mathcal{H}_\infty AW_e$ anti-windup and designed anti-windup AW_ϕ cases

A roll solicitation of 40 deg at time $t = 1$ s followed by a step of –60 deg at time $t = 15$ s and a step of +60 deg at time $t = 30$ s is considered to compare the results. The time responses of the roll angle for the case without saturation, with the $\mathcal{H}_\infty AW_e$ anti-windup resulting from [7] and the designed dynamic AW_ϕ anti-windups are plotted in Figure 7. Similarly, the time evolutions of the control input δ_{pc} in these cases are depicted in Figure 8.

One can observe that the level of performance of the very well-tuned $\mathcal{H}_\infty AW_e$ anti-windup is slightly degraded in comparison with the two cases of AW_ϕ design, but it remains acceptable and close to the ideal response that would be obtained if no saturation was present in the actuator block. One can also remark that the dynamic anti-windup design makes it possible to speed-up the rising time (less than 6 seconds) toward the set-point, with respect to the static anti-windup design (more than 6 seconds), even with very basic anti-windup dynamics (AW_ϕ design 1).

Complementary illustrations

The rate-saturation effectiveness is illustrated in Figures 9 and 10, where the signals v and $\dot{x}_a$ are plotted, respectively, for the case with and without anti-windup. One can check that the anti-windup action both reduces the number of rate-saturation events and the amplitude of the signal v entering the saturation element (see Equation (3)).

Moreover, the stick response of the system, *i.e.*, the output of the pilot gain block, is plotted in Figure 11 to illustrate the efficiency of the anti-windup design. In this case, with a moderately aggressive pilot ($K_{pil} = 2$), one can check that the pilot workload increases in

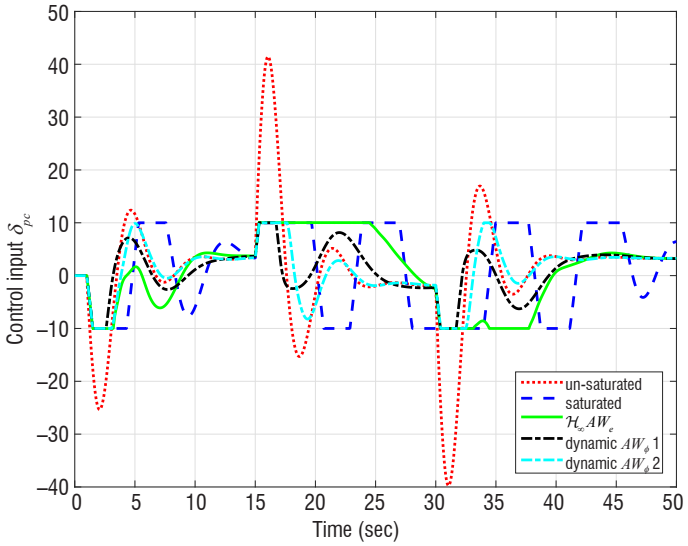


Figure 8 – roll solicitation of +40 deg at time $t = 1$ s followed by a step of –60 deg at time $t = 15$ s and a step of +60 deg at time $t = 30$ s: comparison of the saturating input for the un-saturated, saturated (no compensation of the saturation), $\mathcal{H}_\infty AW_e$ anti-windup and designed anti-windup AW_ϕ cases

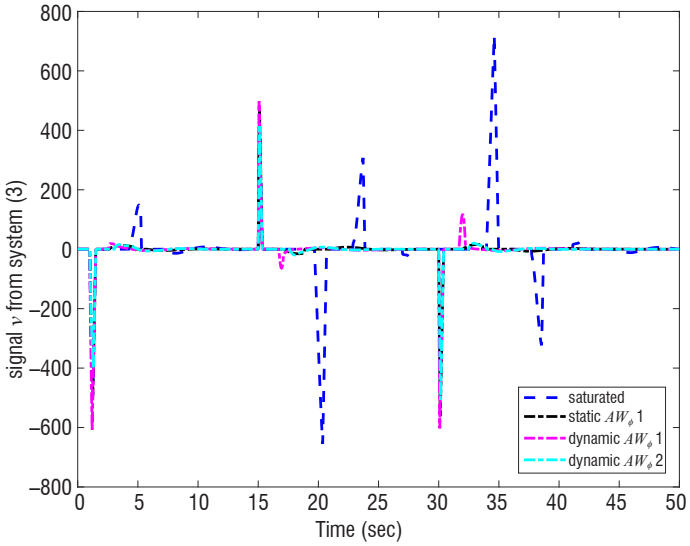


Figure 9 – roll solicitation of +40 deg at time $t = 1$ s followed by a step of –60 deg at time $t = 15$ s and a step of +60 deg at time $t = 30$ s: comparison of the signal v used in Equation (3) for the saturated (no compensation of the saturation) and designed static and anti-windup cases

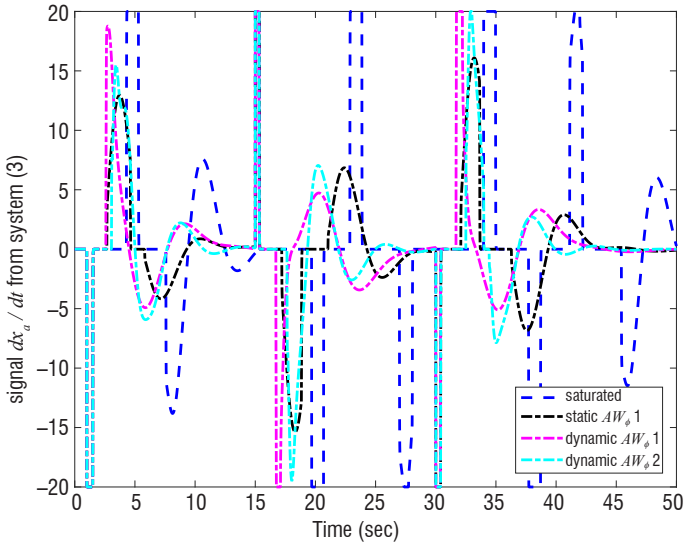


Figure 10 – roll solicitation of +40 deg at time $t = 1$ s followed by a step of –60 deg at time $t = 15$ s and a step of +60 deg at time $t = 30$ s: comparison of the signal $\dot{x}_a$ used in Equation (3) for the saturated (no compensation of the saturation) and designed static and anti-windup cases

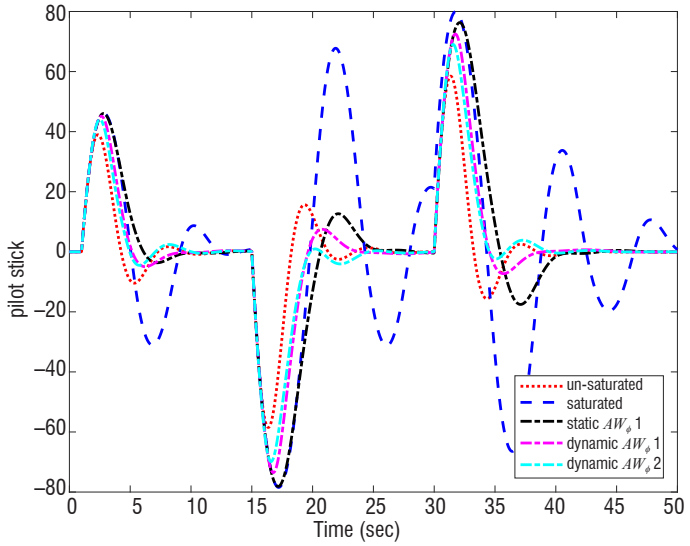


Figure 11 – roll solicitation of +40 deg at time $t = 1$ s followed by a step of –60 deg at time $t = 15$ s and a step of +60 deg at time $t = 30$ s: comparison of the pilot stick output for the un-saturated, saturated (no compensation of the saturation) and designed static and anti-windup cases

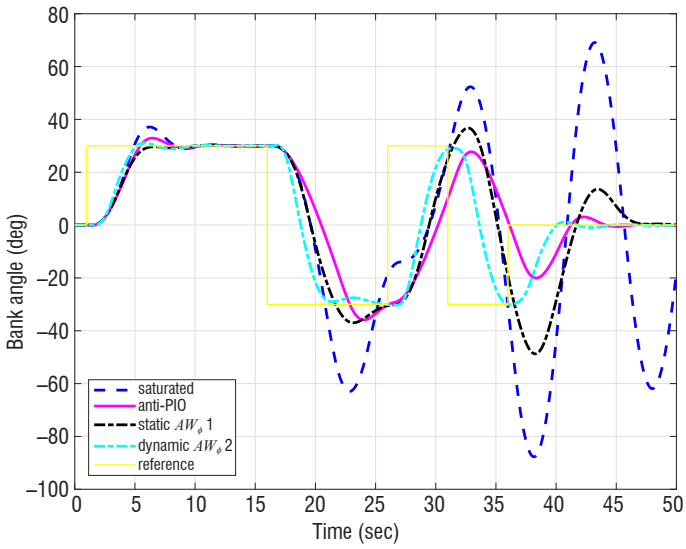


Figure 12 – roll solicitation with a 3211 type input of amplitude $\pm$ 30 deg with a $\Delta t = 5$ s: comparison between the performance outputs for the saturated (no compensation of the saturation), standard anti-PIO and designed static and anti-windup cases

the presence of saturation, and returns to the order of magnitude of the unsaturated case when anti-windup actions are present. Note also that when a more aggressive pilot is investigated (not shown here), with $K_{pil} = 3$, the saturated system becomes instable as soon as no anti-windup is present, but its stability is preserved in the presence of static or dynamic anti-windup actions.

Finally, the time evolution of the fourth bank-angle output (roll angle) in response to a 3211 type input is shown in Figure 12 for various configurations (with or without anti-windup). This type of input allows to effectively excite the aircraft modes of motion. The time unit Δt is set to 5 s to generate sufficient excitation in the aircraft modes of motion.

This illustrates the situation where strong excitation of the lateral aircraft modes of motion may result in the instability of the saturation response. Anti-PIO and anti-windup strategies allow stability to be preserved. Moreover, the dynamic anti-windup strategy enables a good tracking of the reference to be preserved, when the standard anti-PIO and the static anti-windup induce degraded responses with overshoot even if stable.

Conclusion

An anti-windup design strategy has been proposed for systems involving both magnitude and rate saturations, and taking into consideration that such saturations elements only affect some of the inputs. Such a situation is illustrated on a lateral flying model of a civil aircraft undergoing moderately aggressive maneuvering by the pilot. For this kind of systems, it is well known that magnitude and rate saturations of the aileron deflection actuator may lead to an undesirable behavior, often called Pilot-Induced-Oscillation (PIO). Anti-windup compensators have been designed through adequate convex optimization schemes, and a comparison with given dynamic anti-PIO filters already developed has also been provided. The numerical evaluation has made it possible to show, first, that a static strategy provides better results than classical anti-PIO filters basically used in industry. Moreover, the increase in the complexity of dynamic anti-windup compensators (both in terms of structure and computation) is compensated by the fact that they make it possible to recover behaviors very close to that which would be obtained if the actuators were linear. In any case, there is room for future work, such as the design of other anti-windup schemes, which may include the parameter-varying approach [21] or reset controllers [25]■

Acronyms

AW (Anti-Windup)
DLAW (Direct Linear Anti-Windup)
LMI (Linear Matrix Inequality)
MRAW (Model Recovery Anti-Windup)
PIO (Pilot-Induced-Oscillation)

References

[1] *Why the Gripen Crashed.* Aerospace America, 32(2):11, 1994.

[2] K. J. ÅSTRÖM, L. RUNDQWIST - *Integrator Windup and how to Avoid it.* American Control Conference, p. 1693-1698, Pittsburgh, PA, 1989.

[3] D.S. BERNSTEIN, A.N. MICHEL - *A Chronological Bibliography on Saturating Actuators.* International Journal of Robust and Nonlinear Control, 5:375-380, 1995.

[4] J-M. BIANNIC, L. BURLION, F. DEMOURANT, G. FERRERES, G. HARDIER, T. LOQUEN, C. ROOS - *SMAC: A Toolbox for Systems Modeling*. Analysis and Control with Matlab/Simulink. Available at: http://w3.onera.fr/smac, 2015.

[5] J-M BIANNIC, C. ROOS - *Introduction to AWAST : The Anti-Windup Analysis and Synthesis Toolbox.* IEEE CACSD Conference, San Antonio, TX, USA, September 2008.

[6] J-M. BIANNIC, S. TARBOURIECH - *Optimization and Implementation of Dynamic Anti-Windup Compensators in Aircraft Control Systems with Multiple Saturations.* Control Engineering Practice, 17(6):703-713, June 2009.

[7] J.-M. BIANNIC, S. TARBOURIECH - *Analyse et ajustement de lois de commande en présence de saturations implantation de filtres anti-PIO générés par synthèse anti-windup.* Technical report, Rapport COCKPIT/OCKF/CO1.1, 2011.

[8] O. BRIEGER, M. KERR, D. LEISSLING, I. POSTLETHWAITE, J. SOFRONY, M. C. TURNER - *Flight Testing of a Rate Saturation Compensation Scheme on the Attas Aircraft.* Aerospace Science and Technology, 13:92-104, 2009.

[9] O. BRIEGER, M. KERR, I. POSTLETHWAITE, M. C. TURNER, J. SOFRONY - *Pilot-Involved-Oscillation Suppression Using Low-Order Antiwindup: Flight-Test Evaluation.* AIAA Journal of Guidance, Control and Dynamics, 35(2):471-483, 2012.

[10] S. GALEANI, S. TARBOURIECH, M. C. TURNER, L. ZACCARIAN - *A Tutorial on Modern Anti-Windup Design.* European Journal of Control, 15(3-4):418-440, 2009.

[11] A. H. GLATTFELDER, W. SCHAUFELBERGER - *Control Systems with Input and Output Constraints.* Springer-Verlag, London, 2003.

[12] P. HIPPE - *Windup in Control. Its Effects and their Prevention.* AIC, Springer, Germany, 2006.

[13] T. HU, Z. LIN - *Control Systems with Actuator Saturation: Analysis and Design.* Birkhäuser, Boston, 2001.

[14] V. KAPILA, K. GRIGORIADIS (Eds.) - *Actuator Saturation Control.* Marcel Dekker, Inc., 2002.

[15] D. H. KLYDE, D. T. MCRUER, T. T. MYERS - *Pilot-Induced Oscillation Analysis and Prediction with Actuator Rate Limiting.* Journal of Guidance, Control and Dynamics, 20(1):81-89, 1997.

[16] B. S. LIEBST, M. J. CHAPA, D. B. LEGGETT - *Nonlinear Prefilter to Prevent Pilot-Induced Oscillations Due to Actuator Rate Limiting.* AIAA Journal of Guidance, Control and Dynamics, 25(4):740-747, 2002.

[17] J. LÖFBERG - *Yalmip - A Toolbox for Modeling and Optimization in Matlab.* Proceedings of the CACSD Conference, Taipei, Taiwan, 2004.

[18] G. PUYOU, J.-M. BIANNIC - *Application of Robust Antiwindup Design to the Longitudinal Aircraft Control to Cover Actuator Loss.* 19th IFAC Symposium on Automatic Control in Aerospace, University of Wurzburg, Germany, September 2013.

[19] I. QUEINNEC, S. TARBOURIECH - *SATAW-Tool - A Saturation Aware Toolbox.* Available at: http://homepages.laas.fr/queinnec/sataw-tool.html, 2012.

[20] I. QUEINNEC, S. TARBOURIECH, G. GARCIA - *Anti-Windup Design for Aircraft Control.* IEEE Conference on Control Applications (CCA), Munich, Germany, 2006.

[21] C. ROOS, J-M. BIANNIC, S. TARBOURIECH, C. PRIEUR, M. JEANNEAU - *On-Ground Aircraft Control Design Using a Parameter-Varying Anti-Windup Approach.* Aerospace Science and Technology, 14(7):459-471, 2010.

[22] L. RUNDQUIST, K. STAHL-GUNNARSSON - *Phase Compensation of Rate-Limiters in Unstable Aircraft.* IEEE Conference on Control Applications, 1996.

[23] H. J. SUSSMANN, E. D. SONTAG, Y. YANG - *A General Result on the Stabilization of Linear Systems Using Bounded Controls.* IEEE Transactions on Automatic Control, 39(12):2411-2425, 1994.

[24] S. TARBOURIECH, G. GARCIA, J. M. GOMES DA SILVA JR., I. QUEINNEC - *Stability and Stabilization of Linear Systems with Saturating Actuators.* Springer, 2011.

[25] S. TARBOURIECH, T. LOQUEN, C. PRIEUR - *Anti-Windup Strategy for Reset Control Systems.* International Journal of Robust and Nonlinear Control, 21(10):1159-1177, 2011.

[26] S. TARBOURIECH, I. QUEINNEC, J.-M. BIANNIC, C. PRIEUR - *Pilot-Induced-Oscillations Alleviation through Anti-Windup Based Approach,* volume VOL TITLE, G. Fasano and J. D. Pinter (eds). Springer, 2016.

[27] S. TARBOURIECH, I. QUEINNEC, M. C. TURNER - *Anti-Windup Design with Rate and Magnitude Actuator and Sensor Saturations.* European Control Conference, Budapest, Hungary, 2009.

[28] S. TARBOURIECH, M. C. TURNER - *Anti-Windup Design: an Overview of Some Recent Advances and Open Problems.* IET Control Theory and Application, 3(1):1-19, 2009.

[29] A. R. TEEL - *Global Stabilization and Restricted Tracking for Multiple Integrators with Bounded Controls.* Systems Control Lett, 18(3):165-171, 1992.

[30] M. C. TURNER, L. ZACCARIAN (Editors) - *Special Issue: Anti-Windup.* International Journal of Systems Science, 37(2):65-139, 2006.

[31] L. ZACCARIAN, A. R. TEEL - *Modern Anti-Windup Synthesis.* Princeton University Press, 2011.



Isabelle Queinnec is currently CNRS researcher at LAAS-CNRS, Toulouse University. She received her PhD degree and HDR degree in automatic control in 1990 and 2000, respectively, from University Paul Sabatier, Toulouse. Her current research interests include constrained control and robust control of processes with limited information, with particular interest in applications on aeronautical systems, robotic, electronic, biochemical and environmental processes. She has been serving as member of the IFAC technical committees on "Biosystems and Bioprocesses" and on "Modelling and Control of Environmental Systems", respectively from 2002 and 2005 and of the IEEE CSS-CEB from 2013. She is currently AE for IET Control Theory and Applications and for the IFAC Journal NAHS (Nonlinear Analysis: Hybrid systems). She is co-author of a book on saturated systems and of more than 50 journal papers, both in control theory and in process engineering.



Sophie Tarbouriech received the PhD degree in Control Theory in 1991 and the HDR degree (*Habilitation à Diriger des Recherches*) in 1998 from University Paul Sabatier, Toulouse, France. Currently, she is full-time researcher (*Directeur de Recherche*) in LAAS-CNRS, Toulouse. Her main research interests include analysis and control of linear and nonlinear systems with constraints (limited information), hybrid dynamical systems. She is currently Associate Editor for IEEE Transactions on Automatic Control, IEEE Transactions on Control Systems Technology, Automatica and European Journal of Control. She is also in the Editorial Board of International Journal of Robust and Nonlinear Control. She is also co-Editor-in-Chief of the French journal JESA (*Journal Européen des Systèmes Automatisés*). Since January 2017, she is Senior Editor of the journal IEEE Control Systems Letters. Since 1999, she is Associate Editor at the Conference Editorial Board of the IEEE Control Systems Society. She is a member of the IFAC Technical Committees on Robust Control and Nonlinear Systems. She is also member of the IEEE Technical Committee on Hybrid Systems.



Jean-Marc Biannic graduated from SUPAERO Engineering School in 1992 and received the PhD degree in Robust Control Theory with the highest honors in 1996 from SUPAERO as well. He joined ONERA as a research scientist in 1997 and received the HDR degree (French habilitation as PhD supervisor) from Paul Sabatier's University of Toulouse in 2010. Jean-Marc Biannic has supervised 6 PhD students. He is the author or co-author of 20 journal papers, beyond 50 conference papers, many book chapters, teaching documents, a tutorial book on multivariable control and Matlab toolboxes. He received in 2011 the second research distinction grade(MR2) from ONERA and the "ERE" distinction from ISAE (Aeronautics and Space Institute) thanks to which he is recognized as a full-professor in PhD committees. Jean-Marc Biannic has participated to several European projects and Garteur Groups (on PIO and nonlinear control). From 2012 to 2016, he has led a research project involving 10 research scientists for the development of the SMAC toolbox (w3.onera.fr/smac) for systems modeling, analysis and control.



Christophe Prieur was born in Essey-les-Nancy, France, in 1974. He graduated in Mathematics from the Ecole Normale Supérieure de Cachan, France in 2000. He received the Ph.D degree in 2001 in Applied Mathematics from the Université Paris-Sud, France, and the "*Habilitation à Diriger des Recherches*" (HDR degree) in 2009. From 2002 he was an associate researcher CNRS at the laboratory SATIE, Cachan, France, and at the LAAS, Toulouse, France (2004-2010). In 2010 he joined the Gipsa-lab, Grenoble, France where he is currently a senior researcher of the CNRS (since 2011). His current research interests include nonlinear control theory, hybrid systems, and control of partial differential equations. He was the Program Chair of the 9th IFAC Symposium on Nonlinear Control Systems (NOLCOS 2013) and of the 14th European Control Conference (ECC 2015). He has been a member of the IEEE-CSS Conference Editorial Board and an associate editor for IMA J. Mathematical Control and Information. He is currently a member of the EUCA-CEB, an associate editor for the IEEE Trans. on Automatic Control, European J. of Control, and IEEE Trans. on Control Systems Technology, and a senior editor for the IEEE Control Systems Letters.